Cell Cycle 13:8, 1313–1326; April 15, 2014; © 2014 Landes Bioscience

Phospho-Bcl-xL(Ser62) influences spindle assembly and chromosome segregation during mitosis

Jianfang Wang[1], Myriam Beauchemin[1], and Richard Bertrand[1,2,*]

[1]Centre de recherche; Centre hospitalier de l'Université de Montréal (CRCHUM) and Institut du Cancer de Montréal; Montréal, Québec, Canada; [2]Département de médecine; Université de Montréal; Montréal, Québec, Canada

Keywords: Bcl-xL, mitosis, PLK1, MAPK14/SAPKp38α, chromosome segregation, spindle-assembly checkpoint, chromosome instability

Abbreviations: Ab, antibody; APC/C, anaphase-promoting complex/cyclosome; Bcl-xl, Bcl2-associated x protein (long isoform) or Bcl2-like protein 1 (long isoform); Bub, budding uninhibited by benzimidazole protein; Cdc, cell division cycle protein; Cdk, cyclin-dependent kinase; CENPA, centromere protein A; CHK1, checkpoint kinase 1; CLIP170, cytoplasmic linker protein 170; DIC, differential interference contrast; FBS, fetal bovine serum; GFP, green fluorescence protein; GSK3, glycogen synthase kinase 3; HA tag, influenza hemagglutinin tag; HEC1, highly expressed in cancer protein 1; H2B, histone 2B; H3, histone 3; JNK, Jun N-terminal kinase; Mad, mitotic arrest deficient protein; MAPK, mitogen-activated protein kinase; MAPKAPK2, mitogen-activated protein kinase-activated protein kinase 2; MPS1, monopolar spindle 1 kinase; PI, propidium iodide; PLK, polo kinase; SAC, spindle-assembly checkpoint; SAPK, stress-activated protein kinase; siRNA, small interfering RNA; wt, wild-type

Functional analysis of a series of phosphorylation mutants reveals that Bcl-xL(Ser62Ala) influences cell entry into anaphase and mitotic exit in taxol-exposed cells compared with cells expressing wild-type Bcl-xL or a series of other phosphorylation mutants, an effect that appears to be independent of its anti-apoptotic activity. During normal mitosis progression, Bcl-xL(Ser62) is strongly phosphorylated by PLK1 and MAPK14/SAPKp38α at the prometaphase, metaphase, and the anaphase boundaries, while it is de-phosphorylated at telophase and cytokinesis. Phospho-Bcl-xL(Ser62) localizes in centrosomes with γ-tubulin and in the mitotic cytosol with some spindle-assembly checkpoint signaling components, including PLK1, BubR1, and Mad2. In taxol- and nocodazole-exposed cells, phospho-Bcl-xL(Ser62) also binds to Cdc20- Mad2-, BubR1-, and Bub3-bound complexes, while Bcl-xL(Ser62Ala) does not. Silencing Bcl-xL expression and expressing the phosphorylation mutant Bcl-xL(Ser62Ala) lead to an increased number of cells harboring mitotic spindle defects including multipolar spindle, chromosome lagging and bridging, aneuploidy with micro-, bi-, or multi-nucleated cells, and cells that fail to resolve undergo mitosis within 6 h. Together, the data indicate that during mitosis, Bcl-xL(Ser62) phosphorylation impacts on spindle assembly and chromosome segregation, influencing chromosome stability. Observations of mitotic cells harboring aneuploidy with micro-, bi-, or multi-nucleated cells, and cells that fail to resolve undergo mitosis within 6 h were also made with cells expressing the phosphorylation mutant Bcl-xL(Ser49Ala) and dual mutant Bcl-xL(Ser49/62Ala).

Introduction

Mitosis involves proper alignment and accurate segregation of sister chromatids into 2 daughter cells to ensure precise inheritance of the genome. Failure of the process can lead to cell death or chromosome instability, aneuploidy, and diseases, including cancer.[1-3] After DNA replication and centrosome duplication, entry into mitosis absolutely requires progressive accumulation of active cyclin B1/Cdk1 complexes in the nucleus that will initiate chromosome condensation, nuclear envelope breakdown, nuclear lamina disassembly, and many forms of nuclear bodies, including Cajal bodies and nucleoli.[4,5] Centrosomes become separated by the end of prophase, and, during prometaphase, highly dynamic mitotic microtubules form bipolar spindles to which chromosomes must be bi-oriented and perfectly aligned by the end of metaphase. The spindle-assembly checkpoint (SAC) is a safety program that ensures the fidelity of chromosome bi-orientation and alignment, controlling entry into anaphase. It is constitutively active until proper microtubule attachment to and tension on kinetochores and individual sister chromatids at centromeric chromosomes.[1-3] Functionally, the SAC negatively regulates the ability of Cdc20 to activate anaphase-promoting complex or

*Correspondence to: Richard Bertrand; Email: richard.bertrand@umontreal.ca
Submitted: 01/09/2014; Revised: 02/13/2014; Accepted: 02/19/2014; Published Online: 03/03/2014
http://dx.doi.org/10.4161/cc.28293

cyclosome (APC/C), as APC/C^{cdc20}. APC/C^{cdc20}, a large multiprotein E3 ubiquitin ligase, targets key mitotic substrates, including cyclinB and securin, provoking entry into anaphase and mitosis conclusion.[6]

The ability of Cdc20 to activate APC/C, evoking entry into anaphase, is tightly regulated by several mechanisms, until all centromeric chromosomes have achieved bipolar kinetochore–microtubule attachment. During prometaphase/metaphase, the established view is that various mitotic checkpoint proteins, including Bub1, BubR1, Bub3, Mad1, and Mad2, bind to kinetochores that lack attachment/tension and generate a "stop anaphase signal" that diffuses into the mitotic cytosol.[7] This "stop anaphase signal" consists of a BubR1- Mad2- and Bub3-bound complex that diffuses into the mitotic cytosol and binds to Cdc20, preventing APC/C activation.[8-12] Direct phosphorylation of Cdc20 by Bub1 and cyclinB1/Cdk1 has also been reported, providing another direct catalytic mechanism that prevents Cdc20 binding to APC/C during SAC.[13]

In recent years, several teams have noted that members of the Bcl-2 family, in addition to their central role in controlling apoptosis during development and cellular stress, also play a part in the cell cycle and DNA repair pathways, effects that are generally distinct from their function in apoptosis and that influence genomic stability.[14,15] Bcl-xL phosphorylation at Ser62 has been detected previously in a variety of cell lines treated with microtubule inhibitors, including nocodazole, paclitaxel, vinblastine, vincristine, colchicine, and pironetin,[16-21] but the exact function of Bcl-xL(Ser62) phosphorylation during mitosis remains elusive. Bcl-xL(Ser62) is located in the unstructured loop domain of the protein, a region generally not essential for its anti-apoptotic function.[22-26] In contrast, a few studies have indicated that a deletion mutant of the loop domain displays an enhanced ability to inhibit apoptosis with no significant alterations in its capacity to bind pro-apoptotic Bax.[22] Some have suggested that Bcl-xL phosphorylation maintains its anti-apoptotic function,[19] while others have reported that phosphorylation causes Bcl-xL to release bound Bax and promote apoptosis.[27] More recently, others have suggested that Bcl-xL phosphorylation impaired its pro-apoptotic N-terminal cleavage.[28] No one has investigated other possible Bcl-xL functions directly impacting mitosis regulation and progression.

To better understand the importance of Bcl-xL phosphorylation events within its flexible loop domain in regulating Bcl-xL functions during cell cycle progression, we generated a series of single-point Bcl-xL cDNA phosphorylation mutants, including Thr41Ala, Ser43Ala, Thr47Ala, Ser49Ala, Ser56Ala, Ser62Ala, and Thr115Ala, and selected stably transfected human cell populations.[25,26] Our first functional screenings were performed in human B lymphoma Namalwa cells, a well-documented and characterized cell line, easily transfected by episomal-expressing vectors that we and others often used in the past to study apoptosis and cell cycle regulation. Validation of the findings of primary screenings was then conducted in wt HeLa cells and HeLa cells with siRNAs and lentivirus expression vectors. In a recent publication, we described the importance of Bcl-xL(Ser49) phosphorylation during telophase and cytokinesis, enabling proper cytokinesis and mitotic exit.[25] In this study, we investigated Bcl-xL(Ser62) phosphorylation and location kinetics during mitosis, tracking the effect of phosphorylation mutant Bcl-xL(Ser62Ala) expression on mitosis progression and chromosome segregation, and deployed siRNAs targeting Bcl-xL expression. We provide evidence that phospho-Bcl-xL(Ser62) is a component of mitosis progression, which appears to be separate from its anti-apoptotic function.

Results

Effect of Bcl-xL and various Bcl-xL phosphorylation mutants on SAC stability and mitosis progression

To examine Bcl-xL's mitotic functions, we generated various HA-tagged Bcl-xL phosphorylation mutants, including Thr41Ala, Ser43Ala, Thr47Ala, Ser56Ala, Ser62Ala, and Thr115Ala, then stably expressed them in Namalwa cells (**Fig. 1A**; **Fig. S1A**). Simple experimental monitoring by flow cytometry with phospho-H3(Ser10) labeling and propidium iodide (PI) staining[29] was undertaken to evaluate the kinetics of total G_2/M (N4 DNA content), early mitotic entry and stability (N4 DNA content, phospho-H3(Ser10)-positive), late mitotic events (N4 DNA content, phospho-H3(Ser10)-negative), G_1 entry (N2 DNA content, phospho-H3[Ser10]-negative), and cell death (sub-G_1 DNA content) in taxol-exposed cells (0.1 μM). Control Namalwa cells (**Fig. 1B**) or Namalwa cells stably transfected with empty vector (**Fig. 1C**) died extensively during taxol treatment (sub-G_1 DNA content; green bars). In contrast, cells stably expressing HA-Bcl-xL and HA-Bcl-xL(Ser62Ala) mutant showed similar strong inhibition of cell death (**Figs. 1D and E**; sub-G_1 DNA content; green bars). Up to 80% of cells overexpressing wild-type (wt) HA-Bcl-xL and HA-Bcl-xL(Ser62Ala) mutants accumulated in early mitosis (N4 DNA/phospho-H3[Ser10]-positive; red bars) at 12 to 24 h during taxol exposure. Interestingly, HA-Bcl-xL-expressing cells started to lose the phospho-H3(Ser10) marker by 36 h, whereas HA-Bcl-xL(Ser62Ala) mutant cells were still stable in early mitosis at 36 h (N4 DNA/phospho-H3[Ser10]-positive; red bars), gradually relinquishing the phospho-H3(Ser10) marker at 48 to 60 h during taxol treatment. The phosphorylation mutants, including HA-Bcl-xL(Thr41Ala), (Ser43Ala), (Thr47Ala), (Ser56Ala), and (Thr115Ala), did not present a phenotype similar to HA-Bcl-xL(Ser62Ala) (**Fig. S1B–F**), revealing the specificity of the HA-Bcl-xL(Ser62Ala) effect on mitosis regulation and progression in taxol-exposed cells. Concomitantly, robust HA-Bcl-xL(Ser62) phosphorylation appeared in taxol-exposed cells in parallel with phospho-H3(Ser10), but not with HA-Bcl-xL(Ser62Ala) mutant (**Fig. 1F**). Together, these results indicated that Bcl-xL(Ser62) phosphorylation occurred in the early phase of mitotic entry and during SAC in taxol-exposed cells. Phospho-Bcl-xL(Ser62) also appeared to influence cell entry into anaphase and mitotic exit. Indeed, failure of this phosphorylation in cells expressing the HA-Bcl-xL(Ser62Ala) mutant maintained taxol-exposed cells in mitosis for a longer time period with no striking difference in cell death rate.

Endogenous Bcl-xL(Ser62) phosphorylation and location in synchronized cells and taxol-sustained SAC in wt HeLa cells

Because the above observations were made in HA-Bcl-xL-transfected and overexpressed cells, we next monitored and explored the role of endogenous phospho-Bcl-xL(Ser62) during normal mitosis. First, human wt HeLa cells were synchronized by double thymidine block and released upon progression to G_2. The cells were then treated with nocodazole (0.35 μM, 4 h), and prometaphase/metaphase cells were collected by mitotic shake-off. A portion of these cells was released from nocodazole

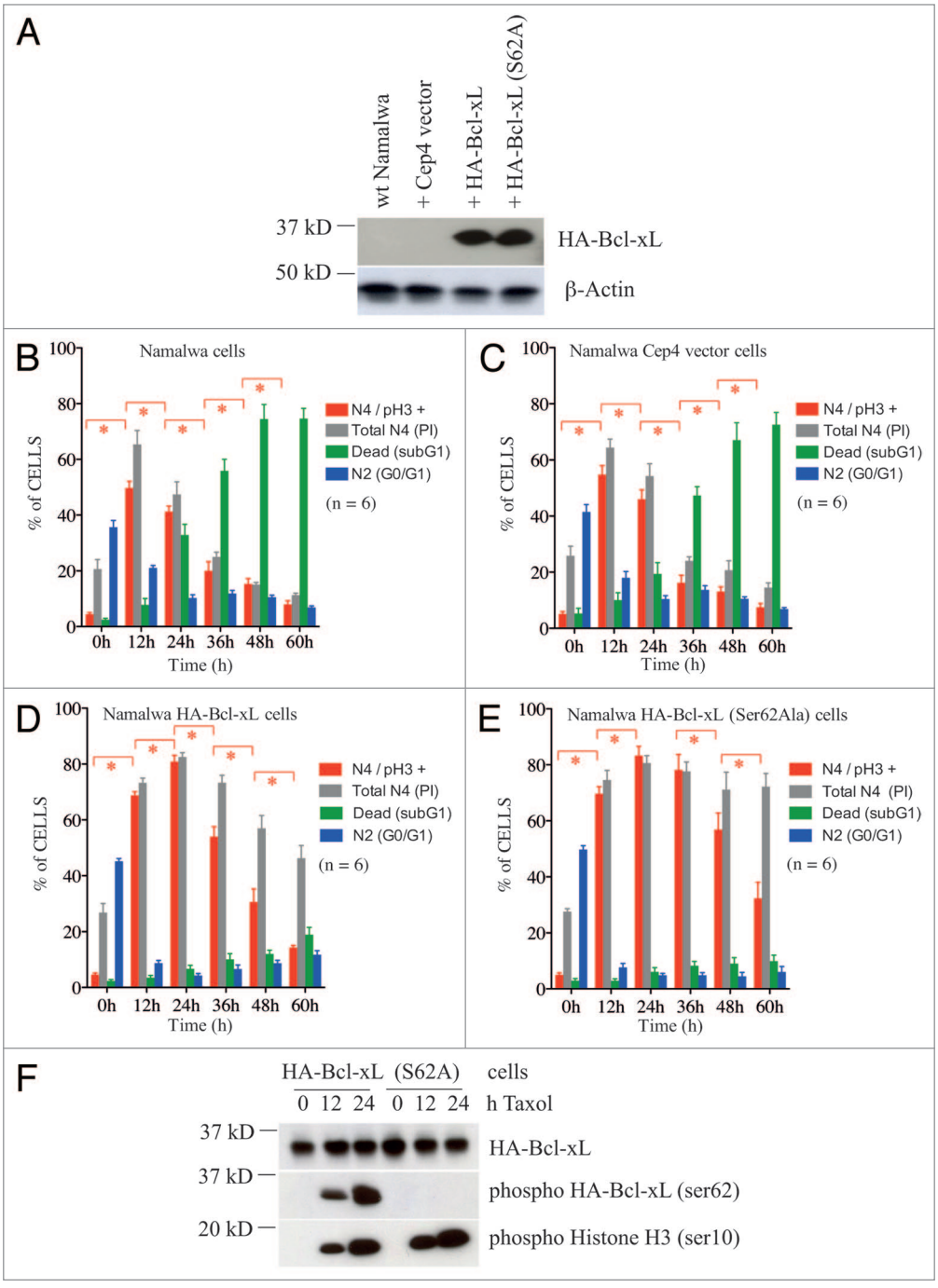

Figure 1. Effect of Bcl-xL and Bcl-xL(Ser62Ala) phosphorylation mutant on SAC stability. (**A**) Expression level of HA-Bcl-xL and Bcl-xL(Ser62Ala) phosphorylation mutant in stably transfected Namalwa cell populations. β-actin expression is shown as control. (**B–E**) Kinetics of total G_2/M (PI staining; gray bars), early mitotic (phospho-H3(Ser10) staining; red bars), dead (PI staining; green bars), and G_1 (PI staining; blue bars) wt Namalwa cells and Namalwa cells expressing empty vector, HA-Bcl-xL, and HA-Bcl-xL(Ser62Ala) phosphorylation mutant during taxol treatment (0.1 μM). Bars represent the means ± s.e.m. of n = 6 independent experiments. Statistical analyses (Student *t* matched-pairs test) are indicated for early mitotic cells (phospho-H3[Ser10] staining; red bars); *Significant ($P < 0.05$). (**F**) Expression and phosphorylation kinetics of HA-Bcl-xL(Ser62) and phospho-H3(Ser10) during taxol treatment (0.1 μM) in Namalwa cells expressing HA-Bcl-xL and Bcl-xL(Ser62Ala) phosphorylation mutant. SDS-PAGE was run on 10% linear gel. Data on additional HA-Bcl-xL phosphorylation mutants are reported in **Figure S1**.

and by growth in the presence of MG-132 (25 μM), a proteasome inhibitor that prevents cyclinB1 and securin destruction, to obtain a cell population at the metaphase/anaphase boundary. A second set was released from nocodazole and by growth in the presence of blebbistatin (10 μM), a selective non-muscle contractile motor myosin II inhibitor that prevents furrow ingression, to attain a cell population at telophase/cytokinesis. A schematic view of these experiments appears in **Figure 2A**. Western blotting disclosed that Bcl-xL was highly phosphorylated at Ser62 at the prometaphase, metaphase, and anaphase boundaries, while it was rapidly de-phosphorylated at telophase/cytokinesis (**Fig. 2B**). Bcl-xL level remained stable along mitosis, and cyclinB1 and phospho-H3(Ser10) expression is shown as specific early mitotic phase markers (**Fig. 2B**). We next looked for phospho-Bcl-xL(Ser62) location in unperturbed, synchronized wt HeLa cells. In these experiments, wt HeLa cells were synchronized by double thymidine block and release upon progression to G_2 and entry into mitosis. The cells were collected at 30 min intervals from 9 to 12 h after double thymidine block and release, providing mitotic cells at all steps of mitosis. Phospho-Bcl-xL(Ser62) did not co-localize with kinetochore structural proteins, including CENPA and HEC1, or the microtubule plus-end tracking-associated protein CLIP170. It co-localized in centrosomes with γ-tubulin at the metaphase and anaphase boundary, and in the mitotic cytosol and spindle midzone with PLK1, but not clearly with the motor protein dynein (**Fig. 2C**). Cell count data and Pearson correlation coefficients appear in **Table S1**, including cell count controls with Bcl-xL Abs.

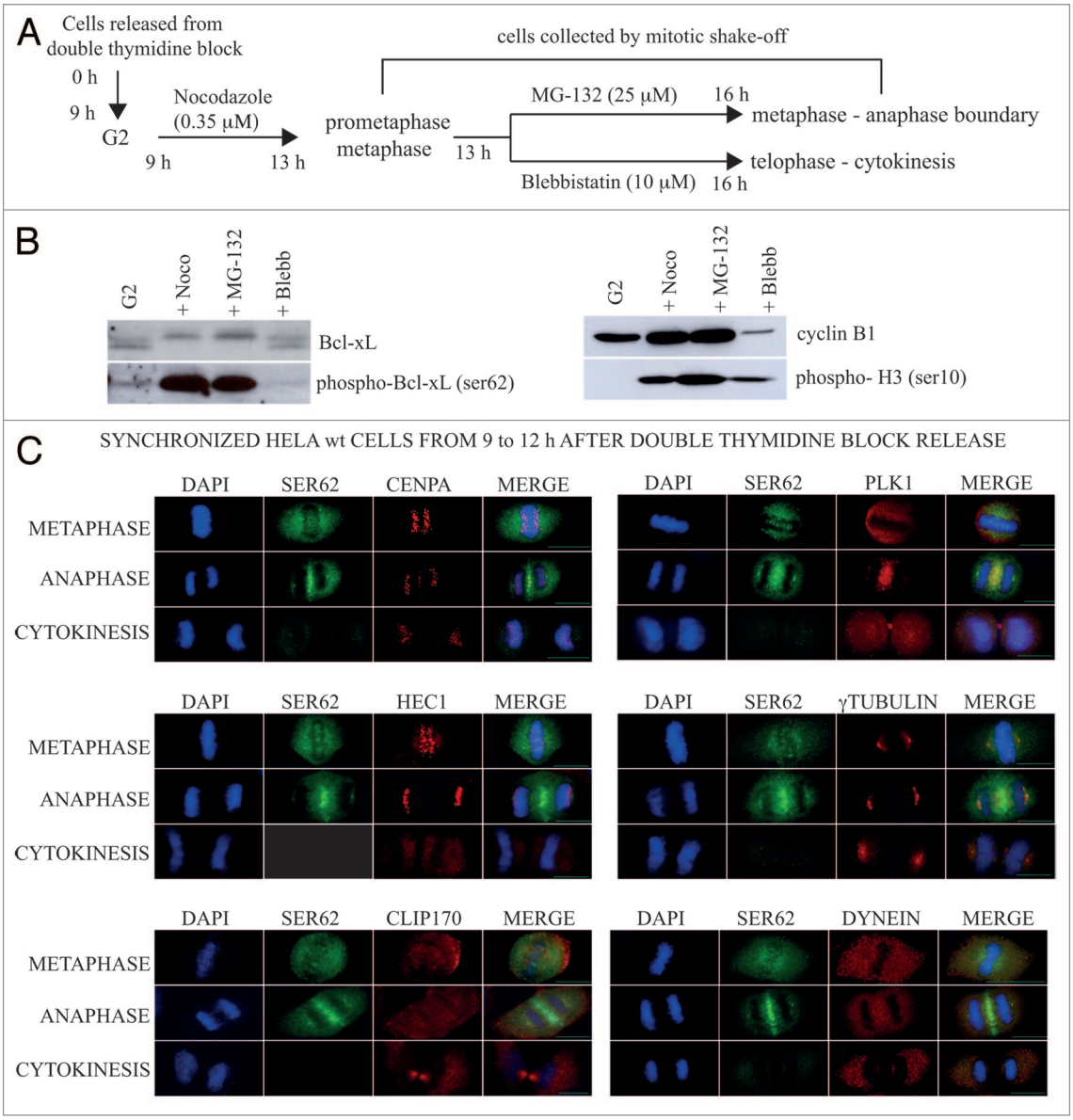

Figure 2. Bcl-xL(Ser62) phosphorylation and location in synchronized wt HeLa cells at mitosis. (**A**) Schematic view of experiments. (**B**) Expression kinetics of Bcl-xL, phospho-Bcl-xL(Ser62), cyclinB1, and phospho-H3(Ser10) in wt HeLa cells obtained at different steps of mitosis. SDS-PAGE was run on 9–18% gradient gels; Bcl-xL Ab was from Origene. (**C**) Co-location of phospho-Bcl-xL(Ser62) with CENPA, HEC1, CLIP170, PLK1, γ-tubulin, and dynein motor protein at different steps of mitosis. Scale bar: 10 μM (inset green line). Cell count data and Pearson's correlation coefficients appear in **Table S1**.

Consistent observations were made in taxol-exposed wt HeLa cells. More than 50 to 60% of wt HeLa cells harbored N4 DNA content and phospho-H3(Ser10) positivity 24 h post-taxol exposure (0.1 μM) (**Fig. S2A**) with Bcl-xL phosphorylation at Ser62 (**Fig. S2B**). The cells gradually lost Bcl-xL(Ser62) phosphorylation with the early mitotic phospho-H3(Ser10) marker. At 24 h after taxol treatment, phospho-Bcl-xL(Ser62) in these cells had a similar location compared with the normal mitosis step at prometaphase and metaphase, with no co-location with kinetochore structural proteins, including CENPA and HEC1, and co-location in centrosomes with γ-tubulin. Interestingly in addition to PLK1, Bcl-xL(Ser62) also co-localizes with some SAC signaling components, including BubR1 and Mad2 in taxol-exposed cells (**Fig. S2C**). Cell count data and Pearson correlation coefficients appear in **Table S1**, including cell count controls with Bcl-xL Abs.

Importance of Bcl-xL(Ser62) for SAC resolution and mitotic exit after microtubule poisoning

As the above experiments and observations revealed a role of Bcl-xL in mitosis progression in normal, unperturbed, proliferative cells, we hypothesized that silencing Bcl-xL expression would have an impact on anaphase entry and length of time for mitotic exit after microtubule poisoning. To perform these experiments, we used nocodazole, a reversible microtubule polymerization inhibitor, which harbors less toxicity than taxol, an irreversible microtubule depolymerization drug, in wt HeLa cells. First, we monitored SAC resolution after 24 h nocodazole treatment (0.35 μM) and release,in cells transfected with control siRNAs or siRNAs targetting Bcl-xL expression. These experiments are illustrated schematically in **Figure 3A**. When Bcl-xL expression was suppressed by 2 independent siRNAs (#2 and #4) (**Fig. 3C and D**), the cells lost phospho-H3(Ser10) labeling more rapidly than those expressing endogenous levels of Bcl-xL (**Fig. 3B**, red bars). Moreover, cells in which Bcl-xL expression was suppressed neither resumed mitosis nor entered into G_1 (**Fig. 3B–D**, blue bars), indicating incompleted cytokinesis and a state of tetraploidy. In gene rescue experiments on HeLa-transduced cells with lentivirus-containing siRNA#2-resistant HA-Bcl-xL (**Fig. 3E**), the kinetics of phospho-H3(Ser10) expression were similar to those in wt HeLa cells (**Fig. 3A**, red bars), with their gradual entry into G_1. Rescue experiments in transduced cells expressing siRNA#2-resistant HA-Bcl-xL(Ser62Ala) (**Fig. 3F**) revealed that these cells maintained a higher level of phospho-H3(Ser10) labeling than cells expressing normal wt Bcl-xL (**Fig. 3B**, red bars) or HA-Bcl-xL (**Fig. 3B**, red bars) levels, with very few of them entering into G_1. Since we previously reported that Bcl-xL is also phosphorylated at Ser49 during telophase and cytokinesis, influencing mitotic exit,[25] experiments on HeLa-transduced cells expressing siRNA#2-resistant HA-Bcl-xL(Ser49Ala) (**Fig. 3G**) and double mutant HA-Bcl-xL(Ser49/62Ala) (**Fig. 3H**) were included. These cells also maintained phospho-H3(Ser10) labeling for a longer period than cells expressing normal wt Bcl-xL (**Fig. 3B**, red bars) or HA-Bcl-xL (**Fig. 3B**, red bars) levels, with few entering into G_1. The kinetics of phospho-H3(Ser10)-only labeling in all these cell populations are summarized in **Figure 3I**, with statistical analysis included as vertical bars on the right (*significant, $P < 0.05$). Bcl-xL, HA-Bcl-xL, HA-Bcl-xL(Ser62Ala), HA-Bcl-xL(Ser49Ala), and HA-Bcl-xL(Ser49/62Ala) expressions under all experimental conditions are reported in **Figure 3J–L**. Other spliced isoforms of Bcl-x gene, including Bcl-xS protein,[30,31] were not detected in HeLa cells (**Fig. 3K and L**). Finally, further microscopy observations revealed accumulation of binucleated cells when Bcl-xL expression was suppressed by 2 independent siRNAs (#2 and #4), indicating cytokinesis failure (**Fig. 3M**). Together, these data are consistent with Bcl-xL functions during SAC and for proper mitotic exit, with Ser62 and Ser49 being important residues.

Live-cell imaging, mitotic spindle defects, and chromosome segregation in cells expressing Bcl-xL phosphorylation mutants

To further investigate the importance of Bcl-xL(Ser62) and (Ser49) for proper mitosis, the kinetics and quality of mitosis progression in proliferating cells were monitored by live-cell microscopy. For this purpose, HeLa cells expressing green fluorescence protein-histone H2B (GFP-H2B) were transduced with lentivirus-containing siRNA#2-resistant HA-Bcl-xL, HA-Bcl-xL(Ser62Ala), HA-Bcl-xL(Ser49Ala), or double mutant HA-Bcl-xL(Ser49/62Ala). Cells were first pre-synchronized at the G_1/S transition by a single thymidine block, and 8 h after block release, green fluorescence images were acquired at 2.6 min intervals for 10 to 12 h, tracking individual cells undergoing mitosis in each cell population. In the first set of experiments (**Fig. 4A**), without silencing endogenous wt Bcl-xL expression, the duration of mitosis (min) of each individual cell was monitored by the time spent from chromatin condensation to cytokinesis and chromatin de-condensation. Each point represents individual cell that succeeded in completing mitosis (**Fig. 4A**). Cell count data of the individual cell harboring multi-polar spindle, or chromosome lagging, or bridging, or cytokinesis failure resulting in micro-, bi-, or multi-nucleated cells, are indicated below the graph. The number of cells that failed to complete their mitosis within 6 h is also indicated. Overall, the percentage of cells harboring various mitotic defects dramatically increased in cells expressing HA-Bcl-xL(Ser62Ala) (36.4%), HA-Bcl-xL(Ser49Ala) (45.0%), and double mutant HA-Bcl-xL(Ser49/62Ala) (54.7%) compared with cells expressing HA-Bcl-xL (16.6%). Interestingly, HA-Bcl-xL overexpression reduced the percentage of cells harboring mitotic defects, in contrast to control wt HeLa cells (16.6% vs. 25.3%). Moreover, mitosis length was significantly longer (significant; $P < 0.001$) in cells expressing double mutant HA-Bcl-xL(Ser49/62Ala) (**Fig. 4A**, top graph). Micrographs illustrating the state of aneuploidy and chromosomal instability with micro-, bi-, or multi-nucleated cells are presented in **Figure S3**.

In a second set of experiments (**Fig. 4B**), endogenous Bcl-xL expression was suppressed with the siRNABcl-xL#2. The effects of silencing Bcl-xL and of expressing siRNA-resistant HA-Bcl-xL and the various HA-Bcl-xL phosphorylation mutants on mitosis duration and the appearance of various mitotic defects were even more dramatic. Indeed, mitosis length was significantly longer (*significant; $P < 0.01$) in cells where endogenous Bcl-xL expression was suppressed, and where the phosphorylation mutants were expressed (**Fig. 4B**, top graph). In addition, the percentage of cells harboring various mitotic defects were increased to 66.2% for HeLa cells treated with siRNA Bcl-xL#2, compared with 23.0%

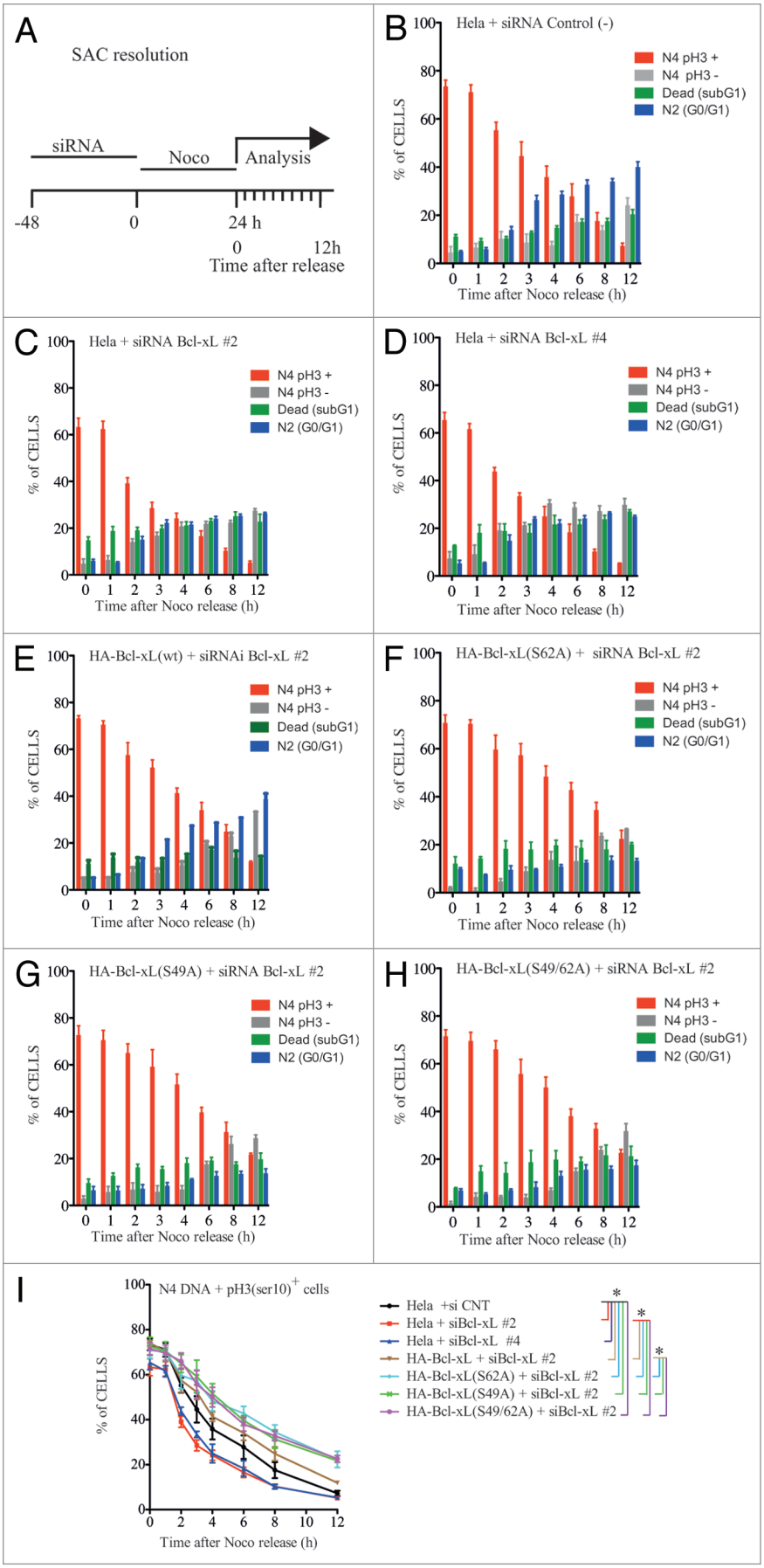

Figure 3A–I. Effect of silencing Bcl-xL expression on SAC stability and resolution. (**A**) Schematic view of experiments where wt HeLa cells and transduced cells expressing siRNA#2-resistant HA-Bcl-xL and various HA-Bcl-xL phosphorylation mutants were transfected with control siRNAs or siRNA#2 or #4 targeting Bcl-xL 48 h prior to nocodazole treatment. After 24 h nocodazole (0.35 μm) exposure, the cells were washed twice and then incubated with fresh medium. Kinetics of early mitotic (N4 DNA content, phospho-H3[Ser10]-positive), late mitotic (N4 DNA content, phospho-H3[Ser10]-negative; gray bars), dead (sub-G_1 cells; green bars), and G_1/G_0 (N2 DNA content; blue bars) (**B**) wt HeLa cells exposed to siRNA control and nocodazole, (**C**) wt HeLa cells exposed to siRNA Bcl-xL#2 and nocodazole, (**D**) wt HeLa cells exposed to siRNA Bcl-xL#4 and nocodazole, (**E**) HeLa cells expressing siRNA#2-resistant HA-Bcl-xL exposed to siRNA Bcl-xL#2 and nocodazole, (**F**) HeLa cells expressing siRNA#2-resistant HA-Bcl-xL(Ser62Ala) exposed to siRNA Bcl-xL#2 and nocodazole, (**G**) HeLa cells expressing siRNA#2-resistant HA-Bcl-xL(Ser49Ala) exposed to siRNA Bcl-xL#2 and nocodazole, and (**H**) HeLa cells expressing siRNA#2-resistant double mutant HA-Bcl-xL(Ser49Ala/Ser62Ala) exposed to siRNA Bcl-xL#2 and nocodazole. Bars represent the means ± s.e.m. of n = 4 experiments. In (**I**), the kinetics of early mitotic cells (N4 DNA content, phospho-H3[Ser10]-positive) from (**B–H**) are plotted together, and statistical analysis (Wilcoxon matched-pairs test) is indicated among the data series by vertical lines at the right; *significant ($P < 0.05$).

for HeLa cells treated with siRNA control, and 29.6% for HeLa cells under siRNA Bcl-xL#2 rescued with HA-Bcl-xL, 68.2% when rescued with HA-Bcl-xL(Ser62A), 81.2% if rescued with HA-Bcl-xL(Ser49A), and 79.5% with the double mutant HA-Bcl-xL(Ser49/62A). The expression levels of Bcl-xL, HA-Bcl-xL, and phosphorylation mutants in HeLa cell populations expressing GFP-H2B are shown in **Figure 4C**. Representative time-lapse video of the live-cell experiments are found as **Movies S1–6**. Together, these data indicate the importance of Bcl-xL(Ser62) phosphorylation for proper chromosome attachment during spindle formation, chromosome segregation, mitosis fidelity, and chromosome stability. Interestingly, cells expressing HA-Bcl-xL(Ser49Ala) showed increased number of individual cells with micro-, bi-, or multi-nucleated cells, consistent with role in cyokinesis.[25]

PLK1 and MAPK14/SAPKp38α are major protein kinases involved in Bcl-xL(Ser62) phosphorylation during mitosis

Based on an in silico consensus site prediction search and known protein kinases

Figure 3J–M. (**J–L**) Bcl-xL and HA-Bcl-xL (wt and mutants) expression kinetics during the time-course of these experiments; β-actin expression is shown as control. SDS-PAGE were run on 9–18% gradient gels; Bcl-xL Ab was from Origene (**J**) and from Cell Signaling (**K and L**). Note: Bcl-xS expression is not detected in HeLa cells. (**M**) Light microscopy of HeLa cells under siRNA BclxL#2 and #4, 36 h post-nocodazole treatment.

activated during mitosis, we first tested a panel of protein kinases by in vitro kinase assays, with purified recombinant human Bcl-xL protein lacking its C-terminal transmembrane domain (rBcl-xL[ΔTM])[24] as substrate (**Fig. 5A**). Among all the kinases tested, PLK1, MAPK8/JNK1, MAPK9/JNK2, MAPKAPK2, MAPK14/SAPKp38α, GSK3α, and GSK3β were positive and able to phosphorylate rBcl-xL(ΔTM) protein at Ser62 in in vitro kinase assays (**Fig. 5A**). Enzyme-specific activities with control substrates are indicated in **Figure S4**, and details of the kinase assays are given in **Table S2**. Then, with specific pharmacological inhibitors and nocodazole-exposed cells, we observed that PLK and MAPK14/SAPKp38α inhibitors reduced HA-Bcl-xL phosphorylation at Ser62 in nocodazole-exposed cells (**Fig. 5B**). A schematic illustration of these experiments, as well as HA-Bcl-xL and phospho-H3(Ser10) expression also appear in **Figure 5B**. Employing a series of specific siRNAs, western blotting of cell extracts collected by mitotic shake-off revealed that the most important kinases involved in Bcl-xL(Ser62) phosphorylation of wt HeLa cells were PLK1 and MAPK14/SAPKp38α (**Fig. 5C**). Indeed, when PLK1 (lane 3) or MAPK14/SAPKp38α (lane 4) expression is silenced, phosphorylation of Bcl-xL(Ser62) was reduced. Silencing MAPKAPK2 (lane 5), MAPK8/JNK1 (lane 6), or MAPK9/JNK2 (lane 7) had no effect on Bcl-xL(Ser62) phosphorylation (**Fig. 5C**), consistent with the experiments using specific pharmacological inhibitors (**Fig. 5B**). These experiments and the expression levels of phospho-Bcl-xL(Ser62), Bcl-xL, phospho-H3(Ser10), PLK1, MAPK14/SAPKp38α, MAPKAPK2, MAPK8/JNK1, MAPK9/JNK2, and β-actin are presented in **Figure 5C**. Additional controls and siRNA experiments are reported in **Figure S5A**, with details in **Table S3**. The data indicate that PLK1 and MAPK14/SAPKp38α are major protein kinases associated with Bcl-xL(Ser62) phosphorylation during early mitosis.

MAPK14/SAPKp38α or PLK1 inhibition in nocodazole-exposed wt HeLa cells reduced phospho-Bcl-xL(Ser62) staining in immunofluorescence experiments (**Fig. 5D**). MAPK14/SAPKp38α inhibition in nocodazole-exposed cells did not impede Bcl-xL(Ser62) co-location with γ-tubulin in centrosomes, while, in contrast, PLK1 inhibition abrogated Bcl-xL(Ser62) co-location with γ-tubulin in centrosomes. These observations are consistent with the known association of PLK1 with centrosomes.[32] In addition, MAPK14/SAPKp38α inhibition reduced phospho-Bcl-xL(Ser62) co-location with Mad2 and with BubR1 in the mitotic cytosol by

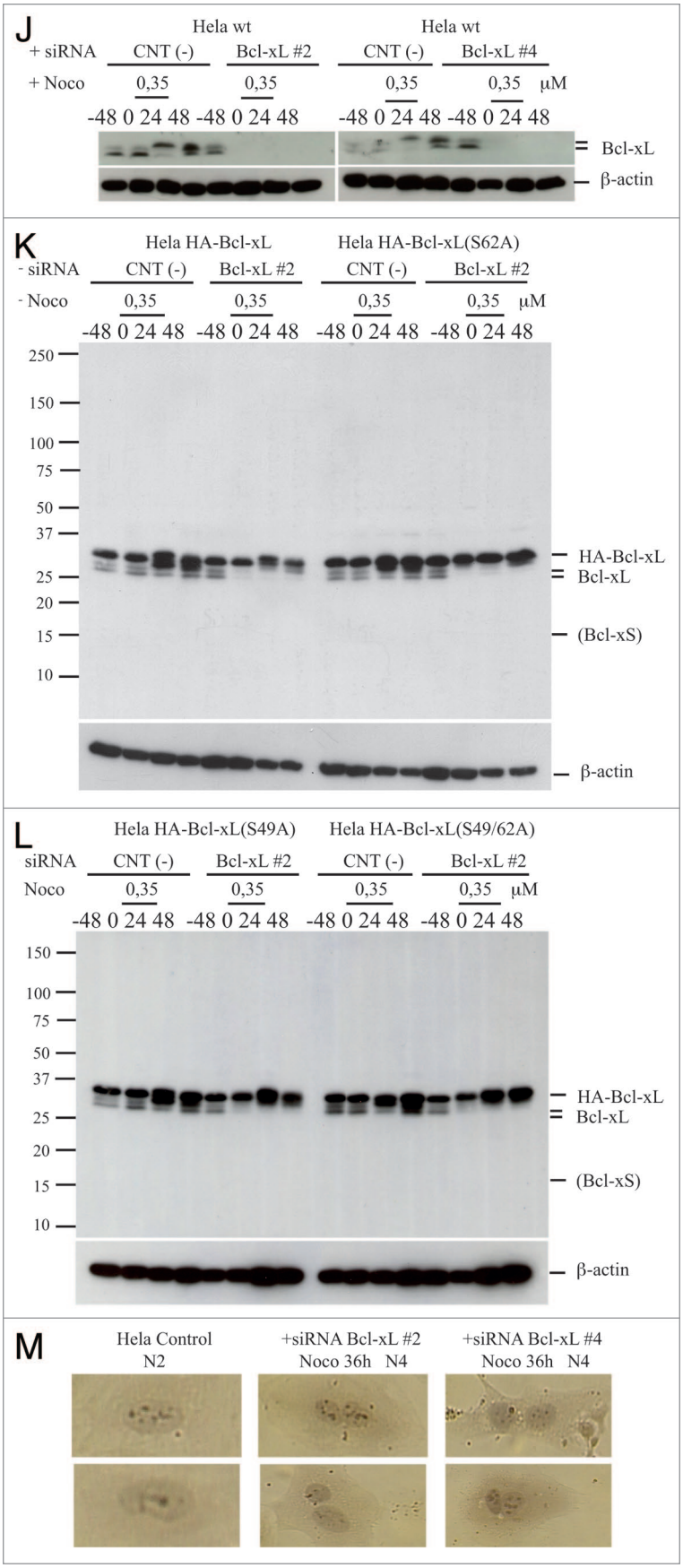

22–25% (Pearson correlation coefficients in **Table S1C**), while PLK1 inhibition retracted Bcl-xL(Ser62) co-location with Mad-2 and BubR1 in mitotic cytosol by approximately 50% (Pearson correlation coefficients in **Table S1C**). Addtional controls for PLK1 and MAPK14/SAPKp38α phosphorylation/activation kinetics in nocodazole-exposed wt HeLa cells and phosphorylation of other known substrates of these enzymes are illustrated in **Figure S5B**.

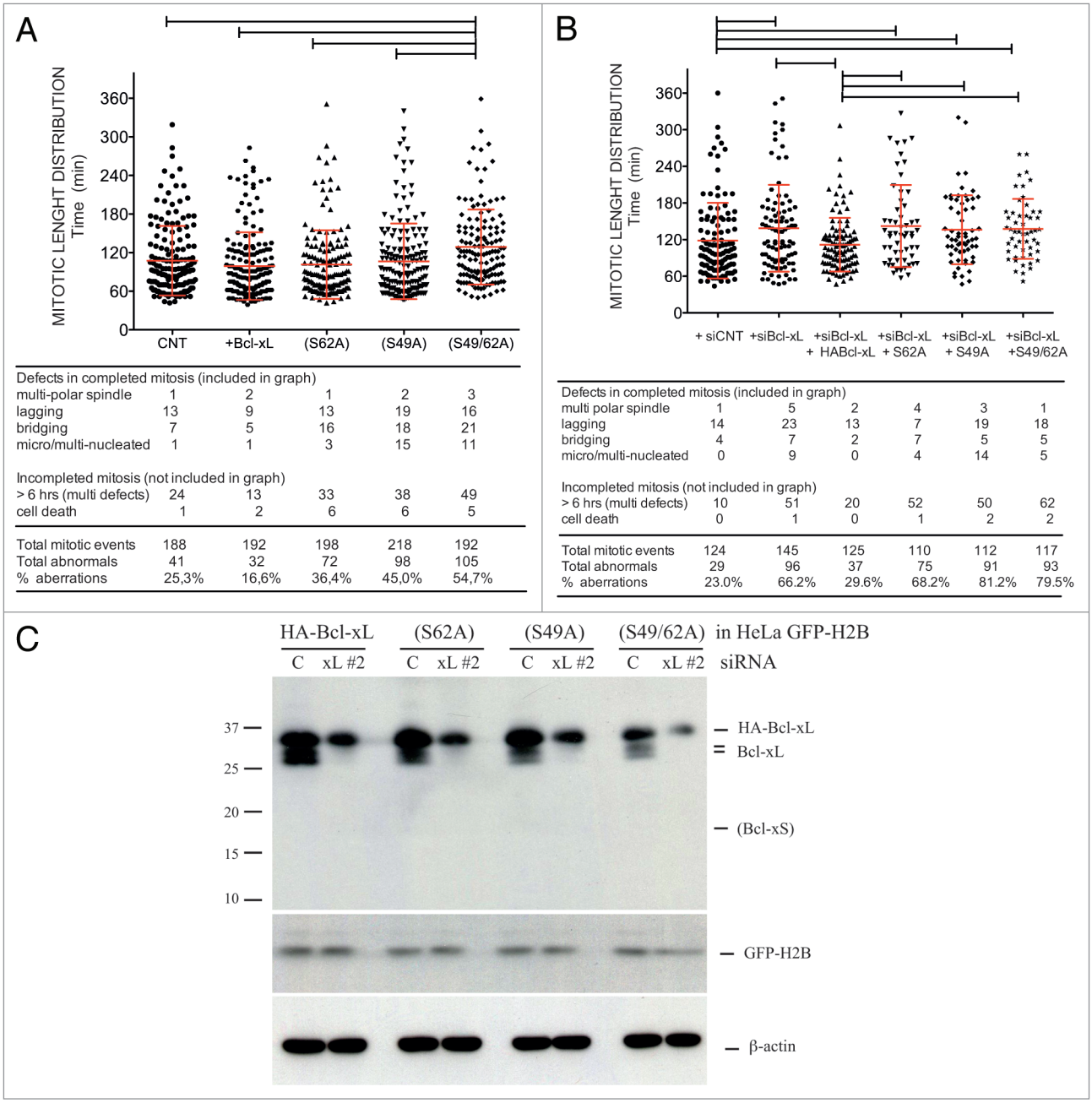

Defects in completed mitosis (included in graph)					
multi-polar spindle	1	2	1	2	3
lagging	13	9	13	19	16
bridging	7	5	16	18	21
micro/multi-nucleated	1	1	3	15	11
Incompleted mitosis (not included in graph)					
> 6 hrs (multi defects)	24	13	33	38	49
cell death	1	2	6	6	5
Total mitotic events	188	192	198	218	192
Total abnormals	41	32	72	98	105
% aberrations	25,3%	16,6%	36,4%	45,0%	54,7%

Defects in completed mitosis (included in graph)						
multi polar spindle	1	5	2	4	3	1
lagging	14	23	13	7	19	18
bridging	4	7	2	7	5	5
micro/multi-nucleated	0	9	0	4	14	5
Incompleted mitosis (not included in graph)						
> 6 hrs (multi defects)	10	51	20	52	50	62
cell death	0	1	0	1	2	2
Total mitotic events	124	145	125	110	112	117
Total abnormals	29	96	37	75	91	93
% aberrations	23.0%	66.2%	29.6%	68.2%	81.2%	79.5%

Figure 4. Time-lapse live-cell imaging. Images from HeLa cells expressing GFP-H2B, HA-Bcl-xL and the phosphorylation (S62A), (S49A), and (Ser49/62A) mutants in (**A**) the absence or (**B**) presence of siRNA Bcl-xL#2 were acquired at 2.6 min intervals for 10 to 12 h at 40× magnification, and image sequences analyzed by tracking individual cells in each cell population to monitor their mitotic behavior. Shown in graphs is the duration of mitosis (min) of each individual cell monitored by the time spent from nuclear envelope breakdown and chromatin condensation to cytokinesis and chromatin de-condensation. Each point represents individual cells monitored in 3 independent experiments, and red bars are means ± s.d. Statistical analyses (Mann–Whitney 2-tailed test) are indicated among the data series by horizontal lines; *significant ($P < 0.001$) in (**A**) and ($P < 0.01$) in (**B**). Cell count data of the individual cell harboring multi-polar spindle, or chromosome lagging, or bridging or cytokinesis failure resulting in micro-, bi-, and multi-nucleated cells, as well as the number of cells that failed to completed their mitosis within 6 h, are indicated below each graph. (**C**) Expression level of Bcl-xL and HA-Bcl-xL and phosphorylation mutants in HeLa cell populations (C, control siRNA; xl#2, Bcl-xL#2 siRNA). GFP-H2B and β-actin expression are shown as control. SDS-PAGE were run on 9–18% gradient gels; Bcl-xL Ab was from from Cell Signaling.

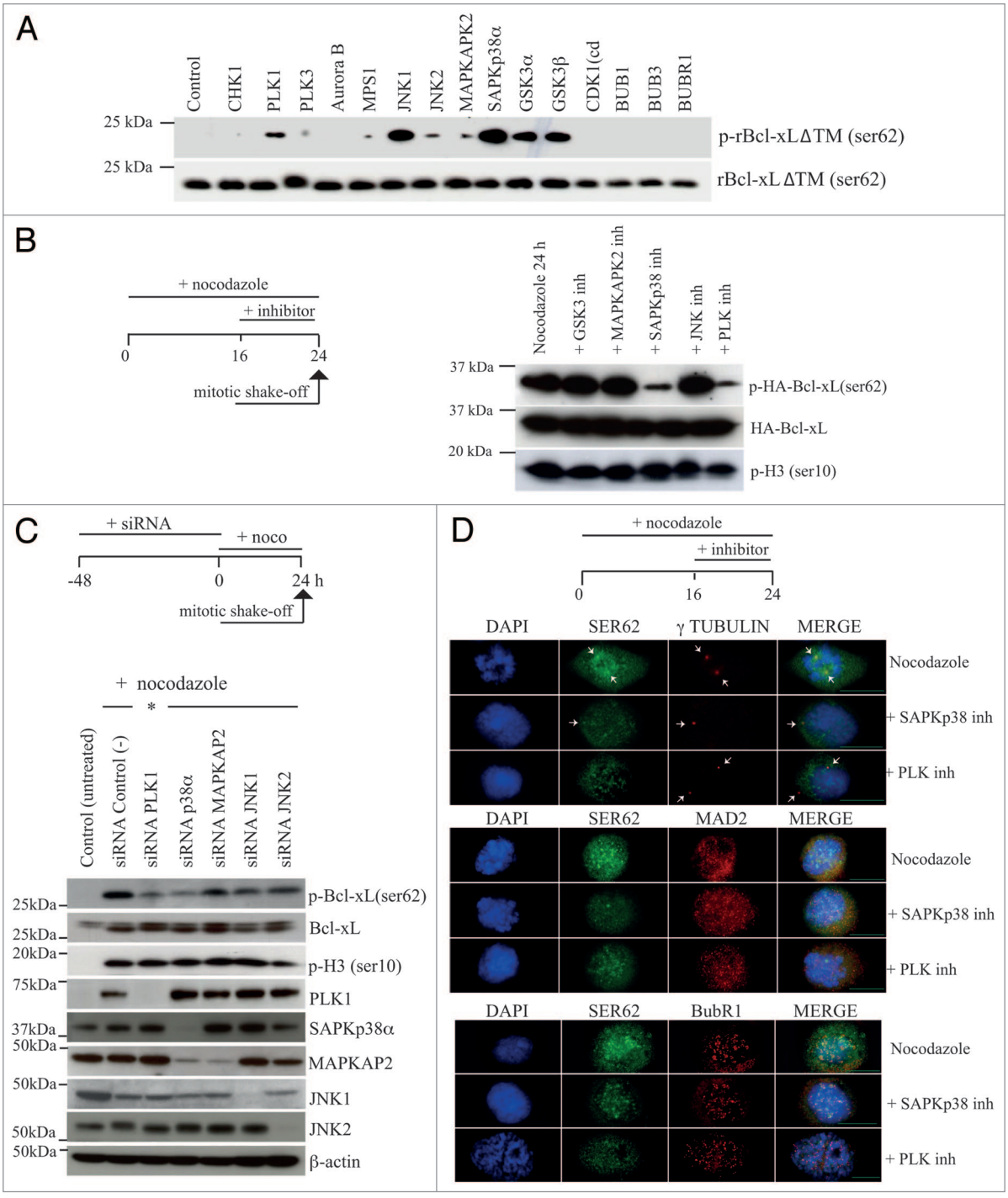

Figure 5. PLK1 and MAPK14/SAPKp38α are major protein kinases involved in Bcl-xL(Ser62) phosphorylation at mitosis. (**A**) In vitro assays of a panel of purified and active protein kinases with recombinant human Bcl-xL(ΔTM) protein as substrate. All enzyme activities were tested on control substrates (**Fig. S4**). Western blots are representative of 2 independent experiments. SDS-PAGE were run on 10% linear gels; Bcl-xL Ab was from BD Science. (**B**) Effects of specific protein kinase inhibitors on Bcl-xL phosphorylation at Ser62 in Namalwa cells exposed to nocodazole. As illustrated on the left, the cells were first exposed to nocodazole (0.35 μM), and, 16 h post-treatment, kinase inhibitors were added for an additional 8 h: GSK3 inhibitor (SB216763, 10 μM); MAPKAPK2 inhibitor (KKALNRQLGVAA, 10 μM); SAPK/p38 inhibitor (SB203580, 2.0 μM); JNK inhibitor (SP600125, 5.0 μM); PLK inhibitor (BI2536, 0.1 μM). The western blots are representative of 3 independent experiments performed with either nocodazole or taxol treatment. SDS-PAGE were run on 10% linear gels. (**C**) Effects of specific siRNAs targeting PLK1, MAPKAPK2, MAPK14/SAPKp38α, MAPK8/JNK1, and MAPK9/JNK2 expression on Bcl-xL(Ser62) phosphorylation in nocodazole-exposed HeLa cells. A schematic view of these experiments is presented on top. Representative western blotting of 3 independent experiments. SDS-PAGE were run on 9–18% gradient gels; Bcl-xL Ab was from Origene. *Note: nocodazole treatment was avoided in these cells, as PLK1 silencing blocked them in early prometaphase/metaphase. (**D**) Phospho-Bcl-xL(Ser62) co-location with γ-tubulin, Mad2, and BubR1, 24 h after nocodazole treatment in the absence or presence of SAPKp38α or PLK inhibitors. Scale bar: 10 μM (inset green line). A schematic view of these experiments is presented on top. Pearson correlation coefficients appear in **Table S1**.

Interaction between phospho-Bcl-xL(Ser62) and the Cdc20/Mad2/BubR1/Bub3 complex

During SAC, a "stop anaphase signal" consisting of Cdc20-, Mad2-, BubR1-, and Bub3-bound complexes in the mitotic cytosol negatively controls APC/C activity. In experiments on transfected Namalwa cells, we observed that HA-Bcl-xL protein co-immunoprecipitated with Mad2, BubR1, Bub3, and Cdc20, but not Bub1, in unperturbed and taxol-exposed cells (24 h), while HA-Bcl-xL(Ser62Ala) mutant was only bound to Mad2 and, to a much lesser extent, Bub3 (**Fig. 6A**). These interactions were lost as the cells gradually progressed into the later stage of mitosis at 48 h during taxol exposure (**Fig. 6A** and see **Fig. 1D**, red bars). A series of reciprocal co-immunoprecipitations confirmed that Mad2, BubR1, and Cdc20 interact with phospho-HA-Bcl-xL(Ser62) (**Fig. 6B**). Cdc27 (APC-3), a subunit of APC, did not co-immunoprecipitate in these experiments. Finally, similar reciprocal co-immunoprecipitation with Mad2, Cdc20, and BubR1 in nocodazole-exposed wt HeLa cells revealed the presence of Bcl-xL(Ser62) within these complexes (**Fig. 6C**).

Discussion

Our study indicates that during prometaphase and metaphase, PLK1 and MAPK14/p38α-mediated Bcl-xL(Ser62) phosphorylation were found in association with the SAC inhibitory Cdc20-Mad2-BubR1-Bub3-bound complexes. PLK1-mediated Bcl-xL(Ser62) phosphorylation is also associated with centrosomes sub-location with γ-tubulin at early mitotic steps. Importantly, phospho-Bcl-xL(Ser62) function in mitosis appears to be separable from Bcl-xL's known role in apoptosis, as Bcl-xL(Ser62Ala) phosphorylation mutant keeps its anti-apoptotic effect but clearly shows different behavior during mitotic progression. Conceptually, by blocking apoptosis of damaged cells, Bcl-xL allows them to undergo cell cycle checkpoint, a time of arrest within the cell cycle that facilitates damage repair. In turn, phospho-Bcl-xL(Ser62) also seems to act directly on the regulation of mitosis.[24-26]

Several findings in our study support a role of Bcl-xL during mitosis. First, cells overexpressing wt Bcl-xL or the phosphorylation mutant Bcl-xL(Ser62Ala) show differences in phospho-H3(Ser10) de-phosphorylation kinetics while retaining N4 DNA content in taxol- and nocodazole-exposed cells. Second, phospho-Bcl-xL(Ser62) phosphorylation and de-phosphorylation kinetics correlate with SAC/On and SAC/Off kinetics. Third, phospho-Bcl-xL(Ser62) binds Cdc20-Mad2-BubR1-Bub3-bound inhibitory complexes, while Bcl-xL(Ser62Ala) does not. Finally, live-cell imaging experiments clearly showed that silencing Bcl-xL expression or re-expressing the phosphorylation mutant Bcl-xL(Ser62Ala) influences mitosis, with cells harboring chromosome alignment defect, kinetochore–microtubule attachment defect, with chromosome lagging and bridging and cytokinesis failure. We recently reported that Bcl-xL phosphorylation at Ser49 is an important step for proper cytokinesis and mitotic exit.[25] The data in this study indicate that, during mitosis, cells lacking Bcl-xL or expressing the phosphorylation mutant Bcl-xL(Ser49Ala) or double mutant Bcl-xL(Ser49/62Ala) also show increased numbers of cells harboring micro-, bi-, or multinucleated cells, consistent with role in cyokinesis.[25] The observations that phospho-Bcl-xL(Ser62) is located at centrosomes during early steps of mitosis, and that phospho-Bcl-xL(Ser49) also located at centrosomes during the G_2 phase of the cell cycle,[25] are consistent with a putative Bcl-xL function influencing centrosome biology and function, although this is not further addressed in this study. **Figure 6D** provides a simple schematic view of these observations. Futher investigations will be required to elucidate how phospho-Bcl-xL(Ser62) and phospho-Bcl-xL(Ser49) act at the molecular level during mitosis.

Bcl-xL phosphorylation at Ser62 has been detected previously in mitotic cells treated with microtubule inhibitors and binders, including nocodazole, paclitaxel, vinblastine, vincristine, colchicine, and pironetin, and a few protein kinases have been proposed to phosphorylate Bcl-xL at Ser62 in microtubule inhibitor-exposed cells.[16-21] Unlike other studies which investigated single protein kinase, we simultaneously probed more than 14 protein kinases in a combination of assays, including in vitro kinase assays, pharmacological inhibitors, and siRNAs. Most importantly, siRNA analysis was performed in a highly enriched mitotic cell population collected by mitotic shake-off to eliminate and avoid contamination or unwanted effects of these protein kinases in the G_2 cell population. Our systemic approach may explain the discrepancy between our work and that of others. Our experiments identified 2 major protein kinases, PLK1 and MAPK14/SAPKp38α, involved in Bcl-xL(Ser62) phosphorylation during mitosis. PLK1 activity is known to be highly regulated in both time and space and has key functions for cell entry into mitosis, SAC regulation, mitotic exit, and cytokinesis.[32-34] MAPK14/SAPKp38α is another major protein kinase activated during mitosis that plays roles during SAC at the metaphase–anaphase transition.[35-37]

The current model of SAC regulation, supported by many studies, indicates that unattached kinetochores generate a "stop anaphase signal" containing the proteins Mad2, BubR1, and Bub3 that diffuse into the mitotic cytosol and sequester Cdc20 to interfere with APC/C activity.[7-12] However, subsequent entry into anaphase requires SAC resolution and APC/C activation by a mechanism that remains poorly understood. SAC resolution or mitotic slippage has often been observed with microtubule poisons,[38-42] and SAC silencing or resolution at least requires ubiquitination, deubiquitination, and proteolysis activities.[43-45] The formation of SAC inhibitory complexes consisting of Cdc20-, Mad2-, BubR1-, and Bub3-bound complexes are highly dynamic, and several intermediates have been resolved in a reconstituted cell-free system.[46] Since we observed interaction between Bcl-xL(ser62) and these Cdc20-Mad2-BubR1-Bub3-bound complexes, it would be interesting to deploy this system with recombinant Bcl-xL protein and combination of phosphorylation mutant and phosphorylation mimetic recombinant Bcl-xL proteins to resolve their actions on the formation, stability, and disassembly of the Cdc20-, Mad2-, BubR1-, and Bub3-bound inhibitory complexes.

The association between anti-apoptotic Bcl-2 or Bcl-xL and genomic stability has previously been suggested in the context

of DNA damage and repair. Indeed, they have been shown to influence nucleotide excision repair,[47] base excision repair,[48] DNA mismatch repair,[49] the Rad51-dependent homologous recombination pathway,[50,51] gene conversion,[52] and the non-homologous end-joining pathway,[53] exerting significant effects on genomic stability. Bcl-xL also shows specific functions during G_2 checkpoint mediated by DNA damage, effects that are independent of its anti-apoptotic role, but which influence genomic stability.[24,25] Previous studies have also revealed Bcl-2 phosphorylation on Thr69, Ser70, and Ser87, residues within the Bcl-2's unstructured loop domain,[22] during mitotic arrest, and on Ser70 during normal transition to mitosis.[54-58] Although not directly verified, Bcl-2 and its phosphorylation during mitosis has been suggested as a guardian for microtubule integrity, monitoring fidelity of chromosome segregation, an effect proposed to be coupled with Bcl-2 function on apoptosis.[59-61] To the best of our knowledge, this is the first observation that phospho-Bcl-xL(Ser62) is associated with chromosome segregation and chromosome stability as a

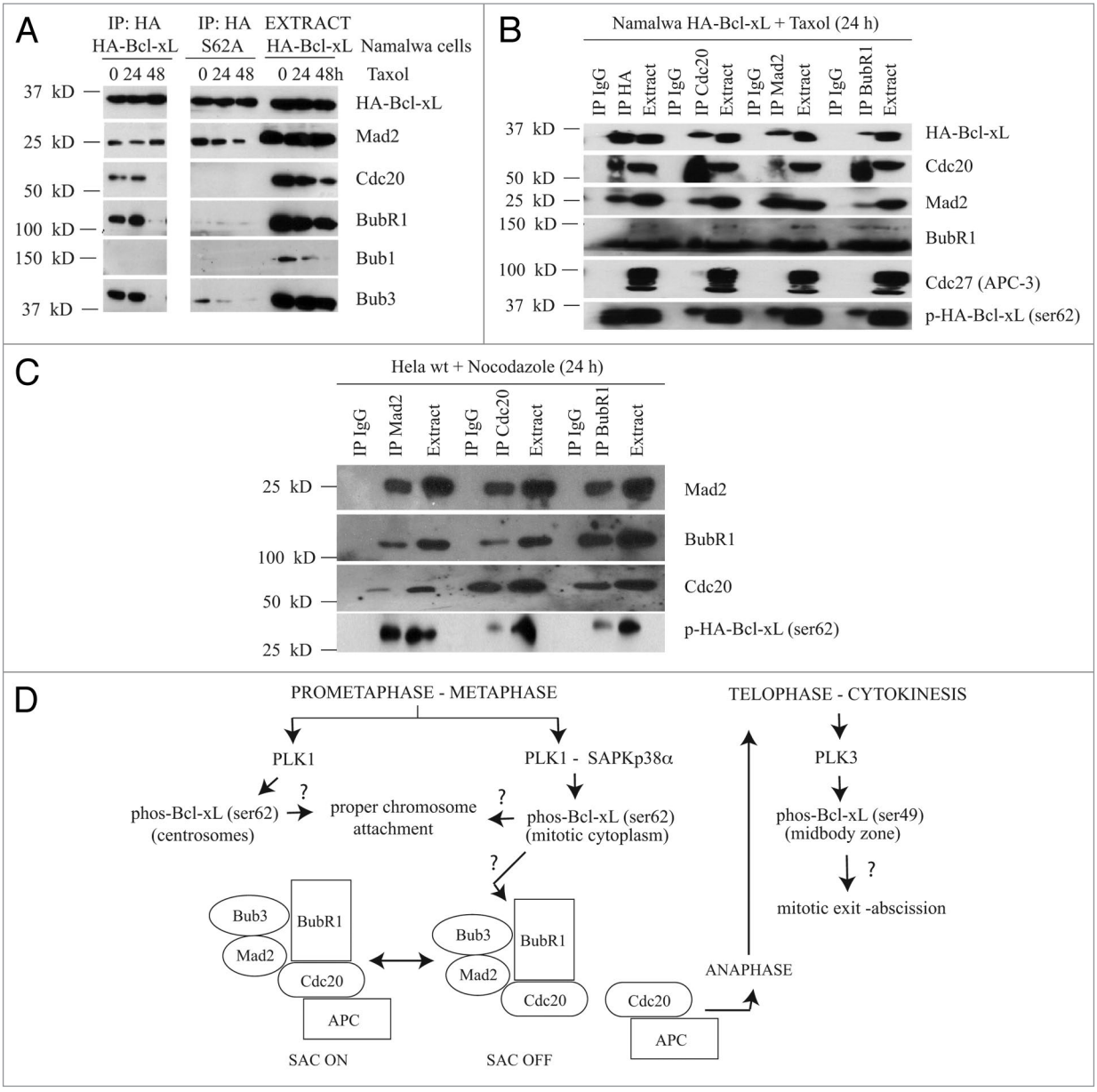

Figure 6. Phospho-Bcl-xL(Ser62) interacts with SAC components. (**A**) Co-immunoprecipitation from Namalwa cells of either HA-Bcl-xL or HA-Bcl-xL(Ser62Ala) mutant protein with Mad2, Cdc20, BubR1, Bub1, or Bub3 in taxol-exposed (0.1 μM) cells. (**B**) Reciprocal co-immunoprecipitation of HA-Bcl-xL and phospho-HA-Bcl-xL(Ser62) with Cdc20, Mad2 and BubR1, but not Cdc27 (APC-3) in taxol-exposed Namalwa cells (0.1 μM, 24 h). IgG represents co-immunoprecipitation experiments with control immunoglobulins. In (**A** or **B**), "Extract" means a protein extract obtained from Namalwa cells expressing HA-Bcl-xL at the indicated time of taxol treatment. Representative of 3 independent experiments. (**C**) Reciprocal co-immunoprecipitation of phospho-Bcl-xL(Ser62) with Mad2, Cdc20, and BubR1 in nocodazole-exposed wt HeLa cells (0.35 μM, 24 h). IgG represents co-immunoprecipitation experiments with control immunoglobulins. In (**C**) "Extract" means a mitotic protein extract obtained from wt HeLa cells after nocodazole treatment (0.1 μM, 24 h). All SDS-PAGE were run on 9–18% gradient gels. (**D**) Schematic view of observations.

consequence of its direct function on mitosis, an effect that appears to be independent of its anti-apoptotic activity. Our finding is in harmony with those observations of others which reveal that dysfunctional mitosis has a dramatic impact on aneuploidy.[62-66]

Materials and Methods

Cell culture, cDNA construction, and cell analysis

Human Namalwa and HeLa cell lines were obtained from American Type Culture Collection and grown at 37 °C under 5% CO_2 in RPMI-1640 medium and DMEM supplemented with 10% heat-inactivated fetal bovine serum (FBS), 100 U/ml penicillin, and 100 μg/ml streptomycin, respectively. The neomycin selected HeLa cell line expressing GFP-histone H2B protein was kindly provided by Dr PS Maddox (Institut de recherche en immunologie et cancer, Université de Montréal).[67] All cDNA constructs, including phosphorylation mutants, were generated as described previously.[25,26] pLenti6.2-DEST vector was obtained from Invitrogen, and lentiviruses were produced in 293FT cells, also from Invitrogen. All vectors were sequenced in both orientations. Transfected Namalwa cells (pCEP4 vectors) and transduced HeLa cells (lentiviruses) were grown under hygromycin B1 (100 μg/ml) and blasticidin (7 μg/ml) selection respectively, to attain stable cell populations prior to the experiments. The kinetics of mitotic entry, cell cycle phase distribution, and cell death were monitored in Coulter EpicsXL flow cytometers with phospho-H3(Ser10) labeling and PI staining. HeLa cells were synchronized by double-thymidine block (2 mM) and release.[25,26]

Protein extraction and immunoblotting

To prepare total protein, cells were extracted with lysis buffer containing 20 mM Hepes- KOH, pH 7.4, 120 mM NaCl, 1% Triton X-100, 2 mM phenylmethylsulfonyl fluoride, a cocktail of protease inhibitors (Complete™, Roche Applied Science, Laval QC) and a cocktail of phosphatase inhibitors (PhosStop™, Roche Applied Science). For immunoprecipitation, the samples were first pre-cleaned with a protein A- and G-Sepharose mixture and, after centrifugation, Abs at 10 μg/ml concentration were incubated at 4 °C for 4 h. All Abs used in this study are listed in **Table S4**. Production and controls of phospho-Bcl-xL(Ser62) and phospho-Bcl-xL(Ser49) Ab specificities have been well documented, both with western blotting and immunostaining.[25,26]

Immunofluorescence microscopy and time-lapse live-cell microscopy

For immunofluorescence microscopy, HeLa cells were seeded and grown directly on coverslips. They were fixed in methanol at –20 °C for 30 min and rapidly immersed in ice-cold acetone for a few seconds. The slides were allowed to dry at room temperature and rehydrated in PBS. Nonspecific binding sites were blocked in PBS containing 5% FBS (blocking solution); then, the slides were incubated sequentially with specific primary Ab (10 μg/ml in blocking solution) and specific labeled secondary Ab (10 μg/ml in blocking solution), followed by DAPI staining, also in blocking solution. All Abs are listed in **Table S4**. Images were generated with a Leica microsystem mounted on a Leica DM6000B microscope and Leica DFC480 camera with Leica Image Manager software, and with a Nikon microsystem mounted on a Nikon Eclipse E600 microscope with a photometric Cool-Snap HQ2 camera and Nikon NIS-Elements software 9 (v 3.8AR). For live-cell imaging, HeLa cells expressing GFP-H2B and the various HA-Bcl-xL constructs (in the presence or absence of specific siRNAs) were pre-synchronized by a single thymidine block. Differential interference contrast (DIC) and/or green fluorescence images were acquired at a 2.6 min interval for 10 to 12 h at 20× or 40× magnification, and image sequences were analyzed by tracking individual cells to track their mitotic behavior. Mitosis duration was monitored by the time spent from nuclear envelope breakdown and chromatin condensation to cytokinesis and chromatin de-condensation. Images were acquired with a Zeiss Axio Observer Z1 automated microscope and analyzed with Axiovision software (v4.8.2).

Protein kinase assays and protein kinase chemical inhibitors

Kinases and kinase assays are described in **Table S2**. Enzyme activities were tested on control substrates and velocities expressed as nmole/min/mg (data in **Fig. S4**). Recombinant human Bcl-xL(ΔTM) protein was produced and purified, as described previously.[24] The protein kinase chemical inhibitors deployed in this study are listed in **Table S2**.

siRNA-mediated protein expression inhibition

HeLa cells were transfected for 48 h with DharmaFECT-1 transfection reagent (ThermoScientific) according to the manufacturer's instructions, with 100 nM of either control siRNA or siRNA targeting different kinases or Bcl-xL (**Table S3**). The cells were then treated 48 h post-transfection with taxol (0.1 μM) or nocodazole (0.35 μM), as indicated, prior to analysis.

Disclosure of Potential Conflicts of Interest

No potential conflicts of interest were disclosed.

Acknowledgments

This work was funded by Grant MOP-97913 from the Canadian Institutes of Health Research to R.B. J.W. received scholarships from the China Scholarship Council (Beijing, China), the Faculté des études supérieures (Université de Montréal, Canada), and the Fondation de l'Institut du cancer de Montréal (Canada). The authors thank Dr Estelle Schmitt (CRCHUM, Canada) for her valuable suggestions and the preparation of Bcl-xL mutant cDNAs, and Dr PS Maddox (Institut de recherche en immunologie et cancer, Canada) for kindly providing the HeLa cell line expressing GFP-H2B protein. The editorial work of Mr Ovid Da Silva is appreciated.

Supplemental Materials

Supplemental materials may be found here:
www.landesbioscience.com/journals/cc/article/28293

References

1. Musacchio A, Salmon ED. The spindle-assembly checkpoint in space and time. Nat Rev Mol Cell Biol 2007; 8:379-93; PMID:17426725; http://dx.doi.org/10.1038/nrm2163
2. Holland AJ, Cleveland DW. Boveri revisited: chromosomal instability, aneuploidy and tumorigenesis. Nat Rev Mol Cell Biol 2009; 10:478-87; PMID:19546858; http://dx.doi.org/10.1038/nrm2718
3. Lara-Gonzalez P, Westhorpe FG, Taylor SS. The spindle assembly checkpoint. Curr Biol 2012; 22:R966-80; PMID:23174302; http://dx.doi.org/10.1016/j.cub.2012.10.006
4. Gavet O, Pines J. Progressive activation of CyclinB1-Cdk1 coordinates entry to mitosis. Dev Cell 2010; 18:533-43; PMID:20412769; http://dx.doi.org/10.1016/j.devcel.2010.02.013
5. Gavet O, Pines J. Activation of cyclin B1-Cdk1 synchronizes events in the nucleus and the cytoplasm at mitosis. J Cell Biol 2010; 189:247-59; PMID:20404109; http://dx.doi.org/10.1083/jcb.200909144
6. Taylor SS, Scott MI, Holland AJ. The spindle checkpoint: a quality control mechanism which ensures accurate chromosome segregation. Chromosome Res 2004; 12:599-616; PMID:15289666; http://dx.doi.org/10.1023/B:CHRO.0000036610.78380.51
7. Cheeseman IM, Desai A. Molecular architecture of the kinetochore-microtubule interface. Nat Rev Mol Cell Biol 2008; 9:33-46; PMID:18097444; http://dx.doi.org/10.1038/nrm2310
8. Li Y, Gorbea C, Mahaffey D, Rechsteiner M, Benezra R. MAD2 associates with the cyclosome/anaphase-promoting complex and inhibits its activity. Proc Natl Acad Sci U S A 1997; 94:12431-6; PMID:9356466; http://dx.doi.org/10.1073/pnas.94.23.12431
9. Fang G, Yu H, Kirschner MW. The checkpoint protein MAD2 and the mitotic regulator CDC20 form a ternary complex with the anaphase-promoting complex to control anaphase initiation. Genes Dev 1998; 12:1871-83; PMID:9637688; http://dx.doi.org/10.1101/gad.12.12.1871
10. Sudakin V, Chan GK, Yen TJ. Checkpoint inhibition of the APC/C in HeLa cells is mediated by a complex of BUBR1, BUB3, CDC20, and MAD2. J Cell Biol 2001; 154:925-36; PMID:11535616; http://dx.doi.org/10.1083/jcb.200102093
11. Tang Z, Bharadwaj R, Li B, Yu H. Mad2-Independent inhibition of APCCdc20 by the mitotic checkpoint protein BubR1. Dev Cell 2001; 1:227-37; PMID:11702782; http://dx.doi.org/10.1016/S1534-5807(01)00019-3
12. Fang G. Checkpoint protein BubR1 acts synergistically with Mad2 to inhibit anaphase-promoting complex. Mol Biol Cell 2002; 13:755-66; PMID:11907259; http://dx.doi.org/10.1091/mbc.01-09-0437
13. Chung E, Chen RH. Phosphorylation of Cdc20 is required for its inhibition by the spindle checkpoint. Nat Cell Biol 2003; 5:748-53; PMID:12855955; http://dx.doi.org/10.1038/ncb1022
14. Schmitt E, Paquet C, Beauchemin M, Bertrand R. DNA-damage response network at the crossroads of cell-cycle checkpoints, cellular senescence and apoptosis. J Zhejiang Univ Sci B 2007; 8:377-97; PMID:17565509; http://dx.doi.org/10.1631/jzus.2007.B0377
15. Danial NN, Gimenez-Cassina A, Tondera D. Homeostatic functions of BCL-2 proteins beyond apoptosis. Adv Exp Med Biol 2010; 687:1-32; PMID:20919635; http://dx.doi.org/10.1007/978-1-4419-6706-0_1
16. Poruchynsky MS, Wang EE, Rudin CM, Blagosklonny MV, Fojo T. Bcl-xL is phosphorylated in malignant cells following microtubule disruption. Cancer Res 1998; 58:3331-8; PMID:9699663
17. Fan M, Goodwin M, Vu T, Brantley-Finley C, Gaarde WA, Chambers TC. Vinblastine-induced phosphorylation of Bcl-2 and Bcl-XL is mediated by JNK and occurs in parallel with inactivation of the Raf-1/MEK/ERK cascade. J Biol Chem 2000; 275:29980-5; PMID:10913135; http://dx.doi.org/10.1074/jbc.M003776200
18. Basu A, Haldar S. Identification of a novel Bcl-xL phosphorylation site regulating the sensitivity of taxol- or 2-methoxyestradiol-induced apoptosis. FEBS Lett 2003; 538:41-7; PMID:12633850; http://dx.doi.org/10.1016/S0014-5793(03)00131-5
19. Du L, Lyle CS, Chambers TC. Characterization of vinblastine-induced Bcl-xL and Bcl-2 phosphorylation: evidence for a novel protein kinase and a coordinated phosphorylation/dephosphorylation cycle associated with apoptosis induction. Oncogene 2005; 24:107-17; PMID:15531923; http://dx.doi.org/10.1038/sj.onc.1208189
20. Tamura Y, Simizu S, Muroi M, Takagi S, Kawatani M, Watanabe N, Osada H. Polo-like kinase 1 phosphorylates and regulates Bcl-x(L) during pironetin-induced apoptosis. Oncogene 2009; 28:107-16; PMID:18820703; http://dx.doi.org/10.1038/onc.2008.368
21. Terrano DT, Upreti M, Chambers TC. Cyclin-dependent kinase 1-mediated Bcl-xL/Bcl-2 phosphorylation acts as a functional link coupling mitotic arrest and apoptosis. Mol Cell Biol 2010; 30:640-56; PMID:19917720; http://dx.doi.org/10.1128/MCB.00882-09
22. Chang BS, Minn AJ, Muchmore SW, Fesik SW, Thompson CB. Identification of a novel regulatory domain in Bcl-X(L) and Bcl-2. EMBO J 1997; 16:968-77; PMID:9118958; http://dx.doi.org/10.1093/emboj/16.5.968
23. Burri SH, Kim CN, Fang G, Chang BS, Perkins C, Harris W, Davis LW, Thompson CB, Bhalla KN. 'Loop' domain deletional mutant of Bcl-xL is as effective as p29Bcl-xL in inhibiting radiation-induced cytosolic accumulation of cytochrome c (cyt c), caspase-3 activity, and apoptosis. Int J Radiat Oncol Biol Phys 1999; 43:423-30; PMID:10030271; http://dx.doi.org/10.1016/S0360-3016(98)00385-X
24. Schmitt E, Beauchemin M, Bertrand R. Nuclear colocalization and interaction between bcl-xL and cdk1(cdc2) during G_2/M cell-cycle checkpoint. Oncogene 2007; 26:5851-65; PMID:17369848; http://dx.doi.org/10.1038/sj.onc.1210396
25. Wang J, Beauchemin M, Bertrand R. Bcl-xL phosphorylation at Ser49 by polo kinase 3 during cell cycle progression and checkpoints. Cell Signal 2011; 23:2030-8; PMID:21840391; http://dx.doi.org/10.1016/j.cellsig.2011.07.017
26. Wang J, Beauchemin M, Bertrand R. Phospho-Bcl-x(L)(Ser62) plays a key role at DNA damage-induced G(2) checkpoint. Cell Cycle 2012; 11:2159-69; PMID:22617334; http://dx.doi.org/10.4161/cc.20672
27. Upreti M, Galitovskaya EN, Chu R, Tackett AJ, Terrano DT, Granell S, Chambers TC. Identification of the major phosphorylation site in Bcl-xL induced by microtubule inhibitors and analysis of its functional significance. J Biol Chem 2008; 283:35517-25; PMID:18974096; http://dx.doi.org/10.1074/jbc.M805019200
28. Arena G, Gelmetti V, Torosantucci L, Vignone D, Lamorte G, De Rosa P, Cilia E, Jonas EA, Valente EM. PINK1 protects against cell death induced by mitochondrial depolarization, by phosphorylating Bcl-xL and impairing its pro-apoptotic cleavage. Cell Death Differ 2013; 20:920-30; PMID:23519076; http://dx.doi.org/10.1038/cdd.2013.19
29. Andreassen PR, Skoufias DA, Margolis RL. Analysis of the spindle-assembly checkpoint in HeLa cells. Methods Mol Biol 2004; 281:213-25; PMID:15220532
30. Boise LH, González-García M, Postema CE, Ding L, Lindsten T, Turka LA, Mao X, Nuñez G, Thompson CB. bcl-x, a bcl-2-related gene that functions as a dominant regulator of apoptotic cell death. Cell 1993; 74:597-608; PMID:8358789; http://dx.doi.org/10.1016/0092-8674(93)90508-N
31. Schmitt E, Paquet C, Beauchemin M, Bertrand R. Bcl-xES, a BH4- and BH2-containing antiapoptotic protein, delays Bax oligomer formation and binds Apaf-1, blocking procaspase-9 activation. Oncogene 2004; 23:3915-31; PMID:15048082; http://dx.doi.org/10.1038/sj.onc.1207554
32. Bruinsma W, Raaijmakers JA, Medema RH. Switching Polo-like kinase-1 on and off in time and space. Trends Biochem Sci 2012; 37:534-42; PMID:23141205; http://dx.doi.org/10.1016/j.tibs.2012.09.005
33. Takaki T, Trenz K, Costanzo V, Petronczki M. Polo-like kinase 1 reaches beyond mitosis--cytokinesis, DNA damage response, and development. Curr Opin Cell Biol 2008; 20:650-60; PMID:19000759; http://dx.doi.org/10.1016/j.ceb.2008.10.005
34. Archambault V, Glover DM. Polo-like kinases: conservation and divergence in their functions and regulation. Nat Rev Mol Cell Biol 2009; 10:265-75; PMID:19305416; http://dx.doi.org/10.1038/nrm2653
35. Takenaka K, Moriguchi T, Nishida E. Activation of the protein kinase p38 in the spindle assembly checkpoint and mitotic arrest. Science 1998; 280:599-602; PMID:9554853; http://dx.doi.org/10.1126/science.280.5363.599
36. Cha H, Wang X, Li H, Fornace AJ Jr. A functional role for p38 MAPK in modulating mitotic transit in the absence of stress. J Biol Chem 2007; 282:22984-92; PMID:17548358; http://dx.doi.org/10.1074/jbc.M700735200
37. Lee K, Kenny AE, Rieder CL. P38 mitogen-activated protein kinase activity is required during mitosis for timely satisfaction of the mitotic checkpoint but not for the fidelity of chromosome segregation. Mol Biol Cell 2010; 21:2150-60; PMID:20462950; http://dx.doi.org/10.1091/mbc.E10-02-0125
38. Ikui AE, Yang CP, Matsumoto T, Horwitz SB. Low concentrations of taxol cause mitotic delay followed by premature dissociation of p55CDC from Mad2 and BubR1 and abrogation of the spindle checkpoint, leading to aneuploidy. Cell Cycle 2005; 4:1385-8; PMID:16138009; http://dx.doi.org/10.4161/cc.4.10.2061
39. Brito DA, Rieder CL. Mitotic checkpoint slippage in humans occurs via cyclin B destruction in the presence of an active checkpoint. Curr Biol 2006; 16:1194-200; PMID:16782009; http://dx.doi.org/10.1016/j.cub.2006.04.043
40. Gascoigne KE, Taylor SS. Cancer cells display profound intra- and interline variation following prolonged exposure to antimitotic drugs. Cancer Cell 2008; 14:111-22; PMID:18656424; http://dx.doi.org/10.1016/j.ccr.2008.07.002
41. Bekier ME, Fischbach R, Lee J, Taylor WR. Length of mitotic arrest induced by microtubule-stabilizing drugs determines cell death after mitotic exit. Mol Cancer Ther 2009; 8:1646-54; PMID:19509263; http://dx.doi.org/10.1158/1535-7163.MCT-08-1084
42. Yang Z, Kenny AE, Brito DA, Rieder CL. Cells satisfy the mitotic checkpoint in Taxol, and do so faster in concentrations that stabilize syntelic attachments. J Cell Biol 2009; 186:675-84; PMID:19720871; http://dx.doi.org/10.1083/jcb.200906150
43. Reddy SK, Rape M, Margansky WA, Kirschner MW. Ubiquitination by the anaphase-promoting complex drives spindle checkpoint inactivation. Nature 2007; 446:921-5; PMID:17443186; http://dx.doi.org/10.1038/nature05734

44. Stegmeier F, Rape M, Draviam VM, Nalepa G, Sowa ME, Ang XL, McDonald ER 3rd, Li MZ, Hannon GJ, Sorger PK, et al. Anaphase initiation is regulated by antagonistic ubiquitination and deubiquitination activities. Nature 2007; 446:876-81; PMID:17443180; http://dx.doi.org/10.1038/nature05694
45. Visconti R, Palazzo L, Grieco D. Requirement for proteolysis in spindle assembly checkpoint silencing. Cell Cycle 2010; 9:564-9; PMID:20081372; http://dx.doi.org/10.4161/cc.9.3.10581
46. Kulukian A, Han JS, Cleveland DW. Unattached kinetochores catalyze production of an anaphase inhibitor that requires a Mad2 template to prime Cdc20 for BubR1 binding. Dev Cell 2009; 16:105-17; PMID:19154722; http://dx.doi.org/10.1016/j.devcel.2008.11.005
47. Liu Y, Naumovski L, Hanawalt P. Nucleotide excision repair capacity is attenuated in human promyelocytic HL60 cells that overexpress BCL2. Cancer Res 1997; 57:1650-3; PMID:9135001
48. Kuo ML, Shiah SG, Wang CJ, Chuang SE. Suppression of apoptosis by Bcl-2 to enhance benzene metabolites-induced oxidative DNA damage and mutagenesis: A possible mechanism of carcinogenesis. Mol Pharmacol 1999; 55:894-901; PMID:10220568
49. Youn CK, Cho HJ, Kim SH, Kim HB, Kim MH, Chang IY, Lee JS, Chung MH, Hahm KS, You HJ. Bcl-2 expression suppresses mismatch repair activity through inhibition of E2F transcriptional activity. Nat Cell Biol 2005; 7:137-47; PMID:15619620; http://dx.doi.org/10.1038/ncb1215
50. Saintigny Y, Dumay A, Lambert S, Lopez BS. A novel role for the Bcl-2 protein family: specific suppression of the RAD51 recombination pathway. EMBO J 2001; 20:2596-607; PMID:11350949; http://dx.doi.org/10.1093/emboj/20.10.2596
51. Dumay A, Laulier C, Bertrand P, Saintigny Y, Lebrun F, Vayssière JL, Lopez BS. Bax and Bid, two proapoptotic Bcl-2 family members, inhibit homologous recombination, independently of apoptosis regulation. Oncogene 2006; 25:3196-205; PMID:16407825; http://dx.doi.org/10.1038/sj.onc.1209344
52. Wiese C, Pierce AJ, Gauny SS, Jasin M, Kronenberg A. Gene conversion is strongly induced in human cells by double-strand breaks and is modulated by the expression of BCL-x(L). Cancer Res 2002; 62:1279-83; PMID:11888891
53. Wang Q, Gao F, May WS, Zhang Y, Flagg T, Deng X. Bcl2 negatively regulates DNA double-strand-break repair through a nonhomologous end-joining pathway. Mol Cell 2008; 29:488-98; PMID:18313386; http://dx.doi.org/10.1016/j.molcel.2007.12.029
54. Ito T, Deng X, Carr B, May WS. Bcl-2 phosphorylation required for anti-apoptosis function. J Biol Chem 1997; 272:11671-3; PMID:9115213; http://dx.doi.org/10.1074/jbc.272.18.11671
55. Basu A, Haldar S. Microtubule-damaging drugs triggered bcl2 phosphorylation-requirement of phosphorylation on both serine-70 and serine-87 residues of bcl2 protein. Int J Oncol 1998; 13:659-64; PMID:9735392
56. Scatena CD, Stewart ZA, Mays D, Tang LJ, Keefer CJ, Leach SD, Pietenpol JA. Mitotic phosphorylation of Bcl-2 during normal cell cycle progression and Taxol-induced growth arrest. J Biol Chem 1998; 273:30777-84; PMID:9804855; http://dx.doi.org/10.1074/jbc.273.46.30777
57. Ling YH, Tornos C, Perez-Soler R. Phosphorylation of Bcl-2 is a marker of M phase events and not a determinant of apoptosis. J Biol Chem 1998; 273:18984-91; PMID:9668078; http://dx.doi.org/10.1074/jbc.273.30.18984
58. Yamamoto K, Ichijo H, Korsmeyer SJ. BCL-2 is phosphorylated and inactivated by an ASK1/Jun N-terminal protein kinase pathway normally activated at G(2)/M. Mol Cell Biol 1999; 19:8469-78; PMID:10567572
59. Haldar S, Basu A, Croce CM. Bcl2 is the guardian of microtubule integrity. Cancer Res 1997; 57:229-33; PMID:9000560
60. Blagosklonny MV, Giannakakou P, el-Deiry WS, Kingston DG, Higgs PI, Neckers L, Fojo T. Raf-1/bcl-2 phosphorylation: a step from microtubule damage to cell death. Cancer Res 1997; 57:130-5; PMID:8988053
61. Blagosklonny MV. Unwinding the loop of Bcl-2 phosphorylation. Leukemia 2001; 15:869-74; PMID:11417471; http://dx.doi.org/10.1038/sj.leu.2402134
62. Bharadwaj R, Yu H. The spindle checkpoint, aneuploidy, and cancer. Oncogene 2004; 23:2016-27; PMID:15021889; http://dx.doi.org/10.1038/sj.onc.1207374
63. Kops GJ, Weaver BA, Cleveland DW. On the road to cancer: aneuploidy and the mitotic checkpoint. Nat Rev Cancer 2005; 5:773-85; PMID:16195750; http://dx.doi.org/10.1038/nrc1714
64. Suijkerbuijk SJ, Kops GJ. Preventing aneuploidy: the contribution of mitotic checkpoint proteins. Biochim Biophys Acta 2008; 1786:24-31; PMID:18472014
65. Fang X, Zhang P. Aneuploidy and tumorigenesis. Semin Cell Dev Biol 2011; 22:595-601; PMID:21392584; http://dx.doi.org/10.1016/j.semcdb.2011.03.002
66. Baker DJ, Dawlaty MM, Wijshake T, Jeganathan KB, Malureanu L, van Ree JH, Crespo-Diaz R, Reyes S, Seaburg L, Shapiro V, et al. Increased expression of BubR1 protects against aneuploidy and cancer and extends healthy lifespan. Nat Cell Biol 2013; 15:96-102; PMID:23242215; http://dx.doi.org/10.1038/ncb2643
67. Maddox PS, Ladouceur AM, Ranjan R, Dorn J, Ratsima H, D'Amours D, Maddox AS. Imaging the mitotic spindle. Methods Enzymol 2012; 505:81-103; PMID:22289449; http://dx.doi.org/10.1016/B978-0-12-388448-0.00013-9